From PS–splines to NURPS

Paul Dierckx and Joris Windmolders

Abstract. A normalized B–spline representation for Powell–Sabin (PS) spline surfaces is extended to piecewise rational surfaces (NURPS). We investigate the adaptation of existing algorithms operating on B–splines to this more general case, the influence of weights and their geometrical interpretation, the possibility of representing planar sections, and the conversion from rational Bézier to NURPS surfaces.

§1. Basic Concepts

1.1. PS–splines

Let $\Omega \subset \mathbb{R}^2$ be a simply connected subset with polygonal boundary $\delta\Omega$. Let Δ be a conforming triangulation of Ω having n vertices V_i with coordinates (u_i, v_i), $i = 1, \ldots, n$, and let Δ^* be a Powell–Sabin (PS) refinement of Δ (see, e.g. [3]), where each triangle $\rho \in \Delta$ is divided into 6 subtriangles. A Powell–Sabin (PS) spline is a piecewise quadratic polynomial with C^1 continuity on Ω. Dierckx [1] shows how to calculate a normalized B–spline basis for PS–splines:

Definition 1. *A PS–spline surface has a normalized B–spline representation*

$$s(u,v) = \sum_{i=1}^{n} \sum_{j=1}^{3} \mathbf{c_{i,j}} B_i^j(u,v), \qquad (u,v) \in \Omega, \tag{1}$$

where $\mathbf{c_{i,j}} = (c_{i,j}^x, c_{i,j}^y, c_{i,j}^z)$ *are the B–spline control points and* $B_i^j(u,v)$ *are the normalized B–splines.*

This representation shares a number of properties with tensor–product B–splines, making it a powerful tool for representing surfaces in CAGD. We summarize the most important properties here. For details we refer to the original paper [1].

Curve and Surface Design: Saint-Malo 1999
Pierre-Jean Laurent, Paul Sablonnière, and Larry L. Schumaker (eds.), pp. 45–54.

ISBN 0-8265-1356-5.

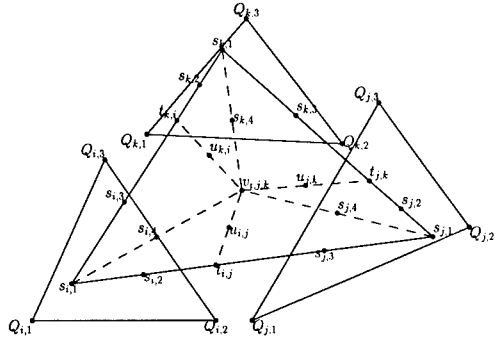

Fig. 1. Domain triangle.

Property 1. $\{B_i^j(u,v)\}_{i=1,\ldots,n}^{j=1,2,3}$ *is a partition of unity:*

$$\begin{cases} B_i^j(u,v) \geq 0, \ (u,v) \in \Omega, \\ \sum_{i=1}^{n} \sum_{j=1}^{3} B_i^j(u,v) \equiv 1, \ (u,v) \in \Omega. \end{cases}$$

Furthermore, $B_{i,j}(u,v)$ is nonzero only on triangles $\rho \in \Delta$ having V_i as a vertex:

Property 2.

$$B_i^j(V_l) = \frac{\partial B_i^j(V_l)}{\partial u} = \frac{\partial B_i^j(V_l)}{\partial v} = 0, \qquad l \neq i. \tag{2}$$

The local control, affine invariance and convex hull properties follow immediately. Linear functions can be represented exactly. In particular, we will make use of the representations

$$u = \sum_{i=1}^{n} \sum_{j=1}^{3} U_{i,j} B_i^j(u,v), \qquad v = \sum_{i=1}^{n} \sum_{j=1}^{3} V_{i,j} B_i^j(u,v)$$

Definition 2. *The PS–triangles* $t_l(Q_{l,1}, Q_{l,2}, Q_{l,3})$, $l = 1, \ldots, n$ *in the planar domain have as vertices the B–spline ordinates* $Q_{l,j}(U_{l,j}, V_{l,j})$, $j = 1, 2, 3$.

Consider a domain triangle $\rho_{i,j,k}(V_i, V_j, V_k) \in \Delta$ with its PS–refinement (see Figure 1). Denote the Bézier ordinates as $s_{v,l}$, $v = i, j, k, l = 1, 2, 3, 4$; $t_{l,m}, u_{l,m}$, $(l,m) \in \{(i,j),(j,k),(k,i)\}$ and $v_{i,j,k}$. They can be written as unique barycentric combinations of the B–spline ordinates:

$$s_{v,l} = \alpha_{v,l} \ Q_{v,1} + \beta_{v,l} \ Q_{v,2} + \gamma_{v,l} \ Q_{v,3}, \tag{3}$$

$$t_{l,m} = \delta_{l,m} \ s_{l,2} + \epsilon_{l,m} \ s_{m,3}, \tag{4}$$

$$u_{l,m} = \delta_{l,m} \ s_{l,4} + \epsilon_{l,m} \ s_{m,4}, \tag{5}$$

$$v_{i,j,k} = \lambda_{i,j,k} \ s_{i,4} + \mu_{i,j,k} \ s_{j,4} + \nu_{i,j,k} \ s_{k,4}. \tag{6}$$

For a given PS–refinement Δ^*, the position of the Bézier ordinates is fixed. This is not the case for the B–spline ordinates. The following lemma however states that there is a restriction on the B–spline ordinates.

Lemma 1. *In order for the basis functions* $\{B_i^j(u,v)\}_{i=1,\ldots,n}^{j=1,2,3}$ *to constitute a partition of unity on* Ω*, it is required that for each vertex* V_i*,* $i = 1,\ldots,n$*, the PS-triangle* $t_i(Q_{i,1}, Q_{i,2}, Q_{i,3})$ *contains the Powell–Sabin points, i.e., the Bézier ordinates* $s_{i,l}, l = 1,2,3,4$*, of any domain triangle having* V_i *as one of its vertices.*

There is a one–one connection between the barycentric coordinates of the Powell–Sabin points at vertex V_i with respect to t_i and the value of the basis functions $B_i^j(u,v)$, $j = 1,2,3$, and of their derivatives at V_i, e.g.

$$B_i^1(V_i) = \alpha_{i,1},\ B_i^2(V_i) = \beta_{i,1},\ B_i^3(V_i) = \gamma_{i,1}. \tag{7}$$

Given a PS–spline surface (1), the corresponding Bézier net can be calculated efficiently by using convex barycentric combinations of the B–spline control points only:

Property 3. *Applying equations (3)–(6) where the ordinates are replaced by control points, yields the corresponding Bézier net of the surface.*

Finally, via the concept of control triangles, the B–spline control points give us valuable insight into the shape of the surface:

Definition 3. *The control triangles are defined as* $T_l(\mathbf{c}_{l,1}, \mathbf{c}_{l,2}, \mathbf{c}_{l,3})$.

Property 4. *Each control triangle* $T_l(\mathbf{c}_{l,1}, \mathbf{c}_{l,2}, \mathbf{c}_{l,3})$ *is tangent to the PS–surface at* $s(V_l)$.

1.2. NURPS

The Normalized B–spline theory for PS–surfaces can now be extended to a rational scheme just like tensor product B–splines are extended to NURBS. Referring to Figure 1, we use the boldface notation for the Bézier points, e.g. $\mathbf{s}_{\mathbf{v},\mathbf{l}}$. Points in homogeneous space get a h–superscript, e.g. $\mathbf{s}^{\mathbf{h}}_{\mathbf{v},\mathbf{l}}$. Their components are $\left(s_{v,l}^{h,x}, s_{v,l}^{h,y}, s_{v,l}^{h,z}, s_{v,l}^{w}\right)$.

Definition 4. *A* Non Uniform Rational Powell–Sabin (NURPS) spline surface *has the form*

$$s(u,v) = \frac{\sum_{i=1}^{n}\sum_{j=1}^{3} \mathbf{c}_{\mathbf{i},\mathbf{j}} w_{i,j} B_i^j(u,v)}{\sum_{i=1}^{n}\sum_{j=1}^{3} w_{i,j} B_i^j(u,v)}, \qquad (u,v) \in \Omega, \tag{8}$$

where $\mathbf{c}_{\mathbf{i},\mathbf{j}} = (c_{i,j}^x, c_{i,j}^y, c_{i,j}^z)$ *are the B–spline control points. We impose that* $w_{i,j} > 0$ *in order for* $s(u,v)$ *to be defined anywhere on* Ω.

If $w_{i,j} = 1$, $i = 1,\ldots,n$, $j = 1,2,3$, then (8) reduces to (1). The following properties are readily verified:

Property 5.

$$s(u,v) = \sum_{i=1}^{n} \sum_{j=1}^{3} \mathbf{c_{i,j}} \phi_i^j(u,v), \tag{9}$$

where

$$\phi_i^j(u,v) = \frac{w_{i,j} B_i^j(u,v)}{\sum_{i=1}^{n} \sum_{j=1}^{3} w_{i,j} B_i^j(u,v)} \tag{10}$$

and

$$\begin{cases} \phi_i^j(u,v) \geq 0, \ (u,v) \in \Omega, \\ \sum_{i=1}^{n} \sum_{j=1}^{3} \phi_i^j(u,v) \equiv 1, \ (u,v) \in \Omega. \end{cases}$$

Furthermore, $\phi_{i,j}(u,v)$ is nonzero only on triangles $\rho \in \Delta$ having V_i as a vertex.

This again implies the local control, affine invariance, and convex hull properties.

Property 6. *A NURPS representation (8) is the 3D–projection in Euclidean space of a 4D PS–spline in homogeneous space:*

$$s(u,v) = \sum_{i=1}^{n} \sum_{j=1}^{3} \mathbf{c^h_{i,j}} B_i^j(u,v), \tag{11}$$

$$\mathbf{c^h_{i,j}} = (w_{i,j} c^x_{i,j}, w_{i,j} c^y_{i,j}, w_{i,j} c^z_{i,j}, w_{i,j}). \tag{12}$$

§2. Evaluation and Subdivision

The evaluation of $s(u,v)$ is performed in two steps:

- First, the corresponding rational piecewise Bézier representation is calculated.
- Then, the rational de Casteljau–algorithm calculates a point on this rational piecewise quadratic Bézier surface. This section shows how to perform the first step in a numerically stable way. For the second step, we refer to Farin [2], Chapter 17.9.

2.1. In homogeneous space

Formulae (3)–(6) can be applied directly in homogeneous space, e.g.

$$\begin{aligned} \mathbf{s^h_{v,l}} &= \alpha_{v,l} \ \mathbf{c^h_{v,1}} + \beta_{v,l} \ \mathbf{c^h_{v,2}} + \gamma_{v,l} \ \mathbf{c^h_{v,3}} \\ &= \left(s^{h,x}_{v,l}, s^{h,y}_{v,l}, s^{h,z}_{v,l}, s^{w}_{v,l} \right) \end{aligned} \tag{13}$$

$$\begin{aligned} \mathbf{v^h_{i,j,k}} &= \lambda_{i,j,k} \ \mathbf{s^h_{i,4}} + \mu_{i,j,k} \ \mathbf{s^h_{j,4}} + \nu_{i,j,k} \ \mathbf{s^h_{k,4}} \\ &= \left(v^{h,x}_{i,j,k}, v^{h,y}_{i,j,k}, v^{h,z}_{i,j,k}, v^{w}_{i,j,k} \right) \end{aligned} \tag{14}$$

Projection back to Euclidean space yields

$$\mathbf{s_{v,l}} = \left(\frac{s^{h,x}_{v,l}}{s^{w}_{v,l}}, \frac{s^{h,y}_{v,l}}{s^{w}_{v,l}}, \frac{s^{h,z}_{v,l}}{s^{w}_{v,l}} \right) \quad \mathbf{v_{i,j,k}} = \left(\frac{v^{h,x}_{i,j,k}}{v^{w}_{i,j,k}}, \frac{v^{h,y}_{i,j,k}}{v^{w}_{i,j,k}}, \frac{v^{h,z}_{i,j,k}}{v^{w}_{i,j,k}} \right).$$

This algorithm has a serious drawback: if the weights vary greatly in magnitude, the coordinates $s^{h,r}_{v,l}, v^{h,r}_{i,j,k}$, $r = x, y, z$ are *blown away*; the calculations don't operate in the convex hull of the control net anymore, and numerical stability is endangered.

2.2. A rational algorithm

The idea behind the rational de Casteljau–algorithm from Farin [2] is to improve numerical stability by rearranging the calculations, avoiding working in homogeneous space:

$$s^{w}_{v,l} = \alpha_{v,l}\ w_{v,1} + \beta_{v,l}\ w_{v,2} + \gamma_{v,l}\ w_{v,3}. \tag{15}$$

Set

$$\tilde{\alpha}_{v,l} = \frac{\alpha_{v,l}\ w_{v,1}}{s^{w}_{v,l}} \geq 0, \quad \tilde{\beta}_{v,l} = \frac{\beta_{v,l}\ w_{v,2}}{s^{w}_{v,l}} \geq 0, \quad \tilde{\gamma}_{v,l} = \frac{\gamma_{v,l}\ w_{v,3}}{s^{w}_{v,l}} \geq 0. \tag{16}$$

Then

$$\mathbf{s_{v,l}} = \tilde{\alpha}_{v,l}\ \mathbf{c_{v,1}} + \tilde{\beta}_{v,l}\ \mathbf{c_{v,2}} + \tilde{\gamma}_{v,l}\ \mathbf{c_{v,3}} \tag{17}$$

with

$$\tilde{\alpha}_{v,l} + \tilde{\beta}_{v,l} + \tilde{\gamma}_{v,l} = 1. \tag{18}$$

The point $\mathbf{s_{v,l}}$ is a convex barycentric combination of $\mathbf{c_{v,1}}, \mathbf{c_{v,2}}$ and $\mathbf{c_{v,3}}$, so numerical stability is guaranteed. Likewise, we find

$$t^{w}_{l,m} = \delta_{l,m}\ s^{w}_{l,2} + \epsilon_{l,m}\ s^{w}_{m,3}, \tag{19}$$

$$u^{w}_{l,m} = \delta_{l,m}\ s^{w}_{l,4} + \epsilon_{l,m}\ s^{w}_{m,4}, \tag{20}$$

$$v^{w}_{i,j,k} = \lambda_{i,j,k}\ s^{w}_{i,4} + \mu_{i,j,k}\ s^{w}_{j,4} + \nu_{i,j,k}\ s^{w}_{k,4}, \tag{21}$$

$$\tilde{\delta}_{l,m} = \frac{\delta_{l,m}\ s^{w}_{l,2}}{t^{w}_{l,m}}, \quad \tilde{\epsilon}_{l,m} = \frac{\epsilon_{l,m}\ s^{w}_{m,3}}{t^{w}_{l,m}}, \tag{22}$$

$$\tilde{\delta}^{*}_{l,m} = \frac{\delta_{l,m}\ s^{w}_{l,4}}{u^{w}_{l,m}}, \quad \tilde{\epsilon}^{*}_{l,m} = \frac{\epsilon_{l,m}\ s^{w}_{m,4}}{u^{w}_{l,m}}, \tag{23}$$

$$\tilde{\lambda}_{i,j,k} = \frac{\lambda_{i,j,k}\ s^{w}_{i,4}}{v^{w}_{i,j,k}}, \quad \tilde{\mu}_{i,j,k} = \frac{\mu_{i,j,k}\ s^{w}_{j,4}}{v^{w}_{i,j,k}}, \quad \tilde{\nu}_{i,j,k} = \frac{\nu_{i,j,k}\ s^{w}_{k,4}}{v^{w}_{i,j,k}}, \tag{24}$$

where

$$\tilde{\delta}_{l,m} + \tilde{\epsilon}_{l,m} = \tilde{\delta}^{*}_{l,m} + \tilde{\epsilon}^{*}_{l,m} = \tilde{\lambda}_{i,j,k} + \tilde{\mu}_{i,j,k} + \tilde{\nu}_{i,j,k} = 1,$$

and finally

$$\mathbf{t_{l,m}} = \tilde{\delta}_{l,m}\ \mathbf{s_{l,2}} + \tilde{\epsilon}_{l,m}\ \mathbf{s_{m,3}}, \tag{25}$$

$$\mathbf{u_{l,m}} = \tilde{\delta}^*_{l,m}\ \mathbf{s_{l,4}} + \tilde{\epsilon}^*_{l,m}\ \mathbf{s_{m,4}}, \tag{26}$$

$$\mathbf{v_{i,j,k}} = \tilde{\lambda}_{i,j,k}\ \mathbf{s_{i,4}} + \tilde{\mu}_{i,j,k}\ \mathbf{s_{j,4}} + \tilde{\nu}_{i,j,k}\ \mathbf{s_{k,4}}. \tag{27}$$

All formulae are convex barycentric combinations operating in the convex hull of the B–spline control net. After having computed the rational Bézier representation, Farin's rational de Casteljau algorithm can be used to evaluate the surface at any point $(u, v) \in \Omega$.

2.3. Subdivision on uniform triangulations

The evaluation and subdivision of spline curves and surfaces are closely related problems. For the particular case of a uniform triangulation Δ, a subdivision scheme for PS–surfaces has been derived [4]. As an application, it was shown how a wireframe of the surface can be calculated in an efficient and numerically stable way. This scheme can easily be extended to NURPS on uniform triangulations again using Farin's technique from the previous section. The details are omitted here.

§3. Control Planes

Recall that the NURPS representation inherits the convex hull, affine invariance, and local control property from the normalized B–spline representation. This section adds the tangent property to the inheritance list, and shows how the rational representation allows for more flexibilty when designing surfaces.

3.1. Tangent property

Referring to the locality of the B–splines (2), it is easy to verify that the evaluation of $s(u, v)$ and its derivatives at vertex V_i yields

$$s(V_i) = \tilde{\alpha}_{i,1}\ \mathbf{c_{i,1}} + \tilde{\beta}_{i,1}\ \mathbf{c_{i,2}} + \tilde{\gamma}_{i,1}\ \mathbf{c_{i,3}}, \tag{28}$$

$$\frac{\partial s(V_i)}{\partial u} = e_{i,1}\ \mathbf{c_{i,1}} + e_{i,2}\ \mathbf{c_{i,2}} + e_{i,3}\ \mathbf{c_{i,3}}, \tag{29}$$

$$\frac{\partial s(V_i)}{\partial v} = d_{i,1}\ \mathbf{c_{i,1}} + d_{i,2}\ \mathbf{c_{i,2}} + d_{i,3}\ \mathbf{c_{i,3}}, \tag{30}$$

for some

$$e_{i,1} + e_{i,2} + e_{i,3} = d_{i,1} + d_{i,2} + d_{i,3} = 0.$$

It follows that the control triangle at V_i is tangent to the surface at $s(V_i)$, i.e., any point $\mathbf{p}$ in the tangent plane is a barycentric combination of the control points $\mathbf{c_{i,1}}, \mathbf{c_{i,2}}, \mathbf{c_{i,3}}$:

$$\mathbf{p} = s(V_i) + a\ \frac{\partial s(V_i)}{\partial u} + b\ \frac{\partial s(V_i)}{\partial v},\ a, b \in \mathbb{R}.$$

This is illustrated in Figure 2 (left).

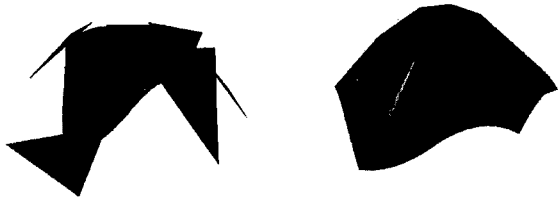

Fig. 2. NURPS surface and its control planes; local planar effects.

3.2. Shape parameters

Farin [2] introduces the concept of shape parameters with respect to rational Bézier curves. A geometric handle allows the designer to influence the shape of the curve in a predictable way, rather than requiring the input of numbers for the weights. In the same work, it is stated that this property does not carry over to rational Bézier surfaces on triangles, but shape parameters can be defined for NURPS.

Recall that $(\tilde{\alpha}_{v,1}, \tilde{\beta}_{v,1}, \tilde{\gamma}_{v,1})$ are the barycentric coordinates of $\mathbf{s_{v,1}}$ with respect to control triangle $T_v(\mathbf{c_{v,1}}, \mathbf{c_{v,2}}, \mathbf{c_{v,3}})$. From (16) it follows that $\mathbf{s_{v,1}}$ can be moved within T_v to a new location $(\tilde{\alpha}'_{v,1}, \tilde{\beta}'_{v,1}, \tilde{\gamma}'_{v,1})$, while keeping its weight $s^w_{v,1}$ constant. The corresponding PS–weights are found immediately as

$$w_{v,1} = \frac{\tilde{\alpha}'_{v,1} s^w_{v,1}}{\alpha_{v,1}}, \quad w_{v,2} = \frac{\tilde{\beta}'_{v,1} s^w_{v,1}}{\beta_{v,1}}, \quad w_{v,3} = \frac{\tilde{\gamma}'_{v,1} s^w_{v,1}}{\gamma_{v,1}} \tag{31}$$

This shows how $(\tilde{\alpha}_{v,1}, \tilde{\beta}_{v,1}, \tilde{\gamma}_{v,1})$ can be used as shape parameters.

3.3. Planar sections

Definition 5. *Let* $[\mathbf{t_1}, \mathbf{t_2}, \ldots, \mathbf{t_n}]$ *denote the* convex hull *of the 3D points* $\mathbf{t_1}, \mathbf{t_2}, \ldots, \mathbf{t_n}$.

Definition 6. *Let* $S(A)$ *denote the image of a subset* $A \subset \Omega$ *under (8).*

Definition 7. *Let* $\tau(a, b, c)$ *denote the* Bézier subtriangle *in the domain plane with vertices* a, b *and* c.

If the control triangles of adjacent vertices V_i, V_j, V_k are chosen to be coplanar, then the surface section $S(\rho_{i,j,k}(V_i, V_j, V_k))$ will be in the same plane, as a consequence of the convex hull property. However, using the weights in the NURPS representation, it is possible to achieve more local planar effects.

The rational evaluation algorithm from Section 2.2 reveals that for $w_{i,1} = w_{i,2} = w_{i,3} = w \to \infty$, $i \in (1, \ldots, n)$ and referring to Figure 1, the following holds on the domain triangle $\rho_{i,j,k}(V_i, V_j, V_k)$:

$$\mathbf{t_{i,j}} = \frac{\delta_{i,j}}{\delta_{i,j} + \frac{\epsilon_{i,j} s^w_{j,3}}{w}} \mathbf{s_{i,2}} + \frac{\frac{\epsilon_{i,j} s^w_{j,3}}{w}}{\delta_{i,j} + \frac{\epsilon_{i,j} s^w_{j,3}}{w}} \mathbf{s_{j,3}}. \tag{32}$$

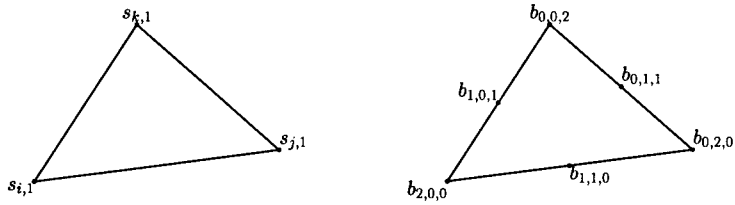

Fig. 3. Bézier triangle.

Thus,

$$\lim_{w\to\infty} \mathbf{t_{i,j}} = \mathbf{s_{i,2}}. \tag{33}$$

Likewise, for the other Bézier points of $\tau\,(s_{i,1}, t_{i,j}, v_{i,j,k})$, we find

$$\mathbf{s_{i,l}} = \alpha_{i,l}\ \mathbf{c_{i,1}} + \beta_{i,l}\ \mathbf{c_{i,2}} + \gamma_{i,l}\ \mathbf{c_{i,3}},\ \ l = 1, 2, 4, \tag{34}$$

$$\lim_{w\to\infty} \mathbf{u_{i,j}} = \lim_{w\to\infty} \mathbf{v_{i,j,k}} = \mathbf{s_{i,4}}. \tag{35}$$

Consequently,

$$S\,(\tau\,(s_{i,1}, t_{i,j}, v_{i,j,k})) = [\mathbf{s_{i,1}}, \mathbf{s_{i,2}}, \mathbf{s_{i,4}}]\,.$$

Similar reasoning on the other Bézier subtriangles shows that

$$\begin{aligned}
S\,(\tau\,(s_{i,1}, v_{i,j,k}, t_{k,i})) &= [\mathbf{s_{i,1}}, \mathbf{s_{i,4}}, \mathbf{s_{i,3}}]\,,\\
S\,(\tau\,(t_{i,j}, s_{j,1}, v_{i,j,k})) &= [\mathbf{s_{i,2}}, \mathbf{s_{i,4}}]\,,\\
S\,(\tau\,(t_{k,i}, v_{i,j,k}, s_{k,1})) &= [\mathbf{s_{i,3}}, \mathbf{s_{i,4}}]\,,\\
S\,(\tau\,(v_{i,j,k}, s_{j,1}, t_{j,k})) &= [\mathbf{s_{i,4}}]\,,\\
S\,(\tau\,(v_{i,j,k}, t_{j,k}, s_{k,1})) &= [\mathbf{s_{i,4}}]\,,
\end{aligned}$$

and therefore,

$$S\,(\rho_{i,j,k}\,(V_i, V_j, V_k)) = [\mathbf{s_{i,1}}, \mathbf{s_{i,2}}, \mathbf{s_{i,4}}, \mathbf{s_{i,3}}] \subset [\mathbf{c_{i,1}}, \mathbf{c_{i,2}}, \mathbf{c_{i,3}}]$$

The latter image is a planar surface section. Figure 2 (right) shows some NURPS surface with very large weights at a vertex.

§4. Conversion from Rational Bézier to NURPS Representation

Suppose we are given a rational quadratic Bézier surface on one domain triangle (see Figure 3) $\rho(s_{i,1}, s_{j,1}, s_{k,1})$

$$b(u,v) = \sum_{i_1+i_2+i_3=2} \mathbf{b}^h_{i_1,i_2,i_3} B^2_{i_1,i_2,i_3}(t_1,t_2,t_3), \tag{36}$$

where $i_1, i_2, i_3 > 0, (u,v) \in \rho$ and (t_1,t_2,t_3) are the barycentric coordinates of (u,v) with respect to ρ. In this section it is shown how a NURPS representation

$$s(u,v) = \sum_{l=i,j,k} \sum_{m=1}^{3} \mathbf{c}^h_{l,m} B^m_l(u,v) \tag{37}$$

of the given surface, for a specific choice of the PS-triangles, is immediately obtained. To simplify the notation, the surfaces are considered in homogeneous space.

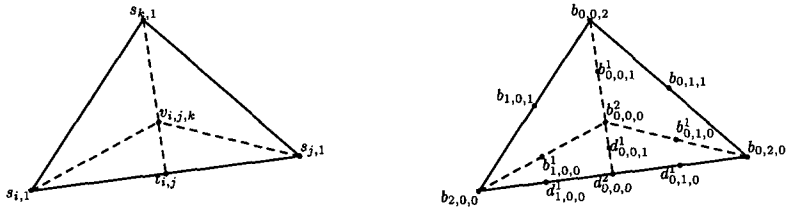

Fig. 4. Subdivision at $v_{i,j,k}$ and $t_{i,j}$.

Lemma 2. *Suppose we are given a triangle* $t(V_i, V_j, V_k)$ *with barycenter* z. *If* W_l *denotes the midpoint of the side opposite to* V_l, *then* $(z + V_l)/2$ *is the barycenter of the triangle* $t(V_l, W_m, W_n)$, $l, m, n \in \{i, j, k\}$, $l \neq m \neq n$.

The construction of the NURPS representation relies on the de Casteljau-algorithm for Bézier triangles (see, e.g., [2]). Subdivision at the barycenter of ρ and at the midpoint of edge $s_{i,1}s_{j,1}$ (see Figure 4) yields the new Bézier points

$$\mathbf{b}^{1,h}_{1,0,0} = \frac{1}{3}\left(\mathbf{b}^h_{2,0,0} + \mathbf{b}^h_{1,1,0} + \mathbf{b}^h_{1,0,1}\right), \tag{38}$$

$$\mathbf{b}^{1,h}_{0,1,0} = \frac{1}{3}\left(\mathbf{b}^h_{1,1,0} + \mathbf{b}^h_{0,2,0} + \mathbf{b}^h_{0,1,1}\right), \tag{39}$$

$$\mathbf{b}^{1,h}_{0,0,1} = \frac{1}{3}\left(\mathbf{b}^h_{1,0,1} + \mathbf{b}^h_{0,1,1} + \mathbf{b}^h_{0,0,2}\right), \tag{40}$$

$$\mathbf{b}^2_{0,0,0} = \frac{1}{3}\left(\mathbf{b}^{1,h}_{1,0,0} + \mathbf{b}^{1,h}_{0,1,0} + \mathbf{b}^{1,h}_{0,0,1}\right), \tag{41}$$

$$\mathbf{d}^{1,h}_{1,0,0} = \frac{1}{2}(\mathbf{b}^h_{2,0,0} + \mathbf{b}^h_{1,1,0}), \tag{42}$$

$$\mathbf{d}^{1,h}_{0,1,0} = \frac{1}{2}(\mathbf{b}^h_{1,1,0} + \mathbf{b}^h_{0,2,0}), \tag{43}$$

$$\mathbf{d}^{1,h}_{0,0,1} = \frac{1}{2}(\mathbf{b}^{1,h}_{1,0,0} + \mathbf{b}^{1,h}_{0,1,0}), \tag{44}$$

$$\mathbf{d}^{2,h}_{0,0,0} = \frac{1}{2}(\mathbf{d}^{1,h}_{1,0,0} + \mathbf{d}^{1,h}_{0,1,0}). \tag{45}$$

After subdivision of the two remaining edges, the 6 subtriangles thus obtained constitute a PS–refinement of ρ, say, with interior point $v_{i,j,k}$ and edge points $t_{i,j}, t_{j,k}, t_{k,i}$ (see Figure 5, left). A NURPS representation of the given surface on this PS–refinement is easily obtained (see Figure 5, right). Set

$$Q_{v,1} = s_{v,1},\ v = i, j, k,$$
$$Q_{i,2} = Q_{j,3} = t_{i,j}, \quad Q_{j,2} = Q_{k,3} = t_{j,k}, \quad Q_{k,2} = Q_{i,3} = t_{k,i},$$

and

$$\mathbf{c}^h_{i,1} = \mathbf{b}^h_{2,0,0},\ \mathbf{c}^h_{i,2} = \mathbf{b}^h_{1,1,0},\ \mathbf{c}^h_{i,3} = \mathbf{b}^h_{1,0,1},$$
$$\mathbf{c}^h_{j,1} = \mathbf{b}^h_{0,2,0},\ \mathbf{c}^h_{j,2} = \mathbf{b}^h_{0,1,1},\ \mathbf{c}^h_{j,3} = \mathbf{b}^h_{1,1,0},$$
$$\mathbf{c}^h_{k,1} = \mathbf{b}^h_{0,0,2},\ \mathbf{c}^h_{k,2} = \mathbf{b}^h_{1,0,1},\ \mathbf{c}^h_{k,3} = \mathbf{b}^h_{0,1,1}.$$

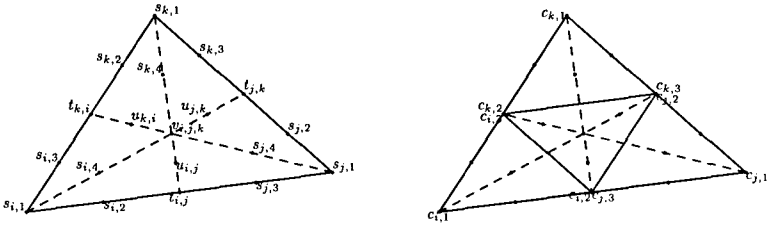

Fig. 5. PS–refinement.

Then by Lemma 2, it follows that the PS–points $s_{v,l}$, $l = 1, 2, 3, 4$ are inside the PS–triangle t_v, $v = i, j, k$. Now recall formula (13) for $v = i, j, k$, and $l = 4$, and formula (14), with $\alpha_{v,4} = \beta_{v,4} = \gamma_{v,4} = \frac{1}{3}$, resp. $\lambda_{i,j,k} = \mu_{i,j,k} = \nu_{i,j,k} = \frac{1}{3}$, in order to calculate the corresponding Bézier points of this NURPS surface. It turns out that these equations are exactly the same as the subdivision formulae (38)–(41). Likewise, since in (3)–(5)

$$(\alpha_{v,2}, \beta_{v,2}, \gamma_{v,2}) = (\frac{1}{2}, \frac{1}{2}, 0),$$
$$(\alpha_{v,3}, \beta_{v,3}, \gamma_{v,3}) = (\frac{1}{2}, 0, \frac{1}{2}),$$
$$(\delta_{l,m}, \epsilon_{l,m}) = (\frac{1}{2}, \frac{1}{2}),$$

for $v = i, j, k$ and $(l, m) \in \{(i, j), (j, k), (k, i)\}$, similar reasoning shows that calculating the corresponding Bézier net of (37) exactly yields the Bézier net of (36) after the proposed subdivisions. Hence, $b(u, v) \equiv s(u, v)$ on ρ.

References

1. Dierckx, P., On calculating normalized Powell–Sabin B–splines, Comput. Aided Geom. Design **15** (1997), 61–78.
2. Farin, G., *Curves and Surfaces for Computer Aided Geometric Design: A Practical Guide*, 4th edition, Academic Press, Boston, 1997.
3. Powell, M. J. D. and M. A. Sabin, Piecewise quadratic approximations on triangles, ACM Trans. Math. Software **3** (1977), 316–325.
4. Windmolders, J., and P. Dierckx, Subdivision of uniform Powell–Sabin splines, Comput. Aided Geom. Design **16** (1999), 301–315.

Paul Dierckx and Joris Windmolders
Celestijnenlaan 200A
3001 Heverlee
Belgium
paul.dierckx@cs.kuleuven.ac.be
joris.windmolders@cs.kuleuven.ac.be